

# Time-Varying Sliding Mode Control for ABS Control of an Electric Car

Sulakshan Rajendran\* Sarah Spurgeon\*\* Georgios Tsampardoukas\*\*\*  
Ric Hampson\*\*\*\*

\*School of Engineering and Digital Arts, University of Kent, UK ( e-mail: [sr602@kent.ac.uk](mailto:sr602@kent.ac.uk))

\*\*Electronic and Electrical Engineering Department, University College London, UK (e-mail: [s.spurgeon@ucl.ac.uk](mailto:s.spurgeon@ucl.ac.uk))

\*\*\* Jaguar Land Rover, W/1/26 Abbey Road, Whitley, Coventry, CV3 4LF, UK

(e-mail: [gtsampar@jaguarlandrover.com](mailto:gtsampar@jaguarlandrover.com), [rhampso2@jaguarlandrover.com](mailto:rhampso2@jaguarlandrover.com))

---

**Abstract:** Controller design for the Anti-Lock Braking System (ABS) of a wheeled vehicle is a challenging task because of the complex and nonlinear nature of the tyre-road interaction. An efficient ABS controller should be capable of maintaining the wheel slip at an optimal value, which is suitable for the particular road conditions experienced at a given instant in time, preventing the wheel from locking while braking. Many controller designs in the literature track either an optimal slip which is assumed constant or are not supported by experimental validation or simulation testing with higher order models. This paper first presents an ABS system based on a conventional Sliding Mode Control (SMC). The performance of this controller is tested on an experimental vehicle. The results are compared with simulation results obtained with both a quarter car model and a full-car model built in the Matlab/Simulink environment. The performance of this controller is improved by effective state estimation using a Sliding Mode Differentiator (SMD) where the results are benchmarked with an implementation using an Extended Kalman Filter (EKF). The paper then presents a controller based on Time-Varying Sliding Mode Control (TV-SMC) which tracks an optimal slip trajectory.

*Keywords:* TV-SMC, ABS control, Vehicle Control, Nonlinear Control.

---

## 1. INTRODUCTION

Increasing environmental concerns regarding CO<sub>2</sub> emissions from conventional vehicles have resulted in increasing interest in the development of Electric or Hybrid Electric Vehicles (EV or HEV). The EV or HEV vehicles are more energy efficient compared to conventional vehicles. Conventional vehicles dissipate more energy converted to heat through friction whereas EV or HEV equipped with regenerative braking can capture some of this wasted energy during braking. The use of regenerative braking systems in EV or HEV vehicles to further reduce energy consumption is of significant interest. The technology thus has the potential to reduce fuel consumption.

ABS systems have been installed in wheeled vehicles for several decades to prevent the wheels from locking during braking thereby ensuring steerability and increased braking performance. This is done by controlling the wheel slip. Slip control allows the braking force to be maximised by maintaining the wheel slip at an optimal value with respect to varying road conditions thus increasing the braking efficiency. During braking, a braking torque is applied to the wheel to reduce the angular velocity. This increases the difference between the reduced linearised wheel velocity and the vehicle velocity which causes the vehicle to skid and this skidding is called wheel slip. The slip varies from minimum

of zero and to a maximum of one. Zero slip implies that the linearised wheel velocity is the same as the vehicle speed and slip of one suggests that the linearised wheel velocity is zero and the wheel is locked but the car is still moving, which corresponds to the vehicle skidding. The installed ABS prevents the wheel locking and improves braking performance. Control of wheel slip dynamics is a challenging problem due to the highly nonlinear and complex nature of the tyre/road interaction. In addition, the system is also subject to external disturbances and parametric uncertainties. Hence, it is required to design a controller which is robust enough to overcome these uncertainties and disturbances. These requirements have motivated the use of SMC control methods for the ABS control problem.

SMC belongs to a well-studied class of discontinuous control and exhibits robustness to unmodeled dynamics, uncertainties and disturbances. Y. Oniz et al (2009) presented an ABS controller based on SMC enhanced by grey-theory. This paper used a grey-predictor to estimate the vehicle velocity and the wheel angular velocity. The proposed controller was tested with a quarter car model and two-wheel lab experimental set up to track a varying optimal slip trajectory. It produced faster convergence and better noise response compared to traditional approaches. Wheel slip control using engine torque control which employs moving sliding surfaces

is presented by K. Chun et al (2004). This only considers tracking a constant optimal slip and it is also assumed to have precise torque sensors. J. Song et al (2005) presented a SMC controller based on an integral sliding surface design for a HEV. E. J. Park et al (2006) presented a conventional SMC for EV with no hydraulics and the brakes are purely controlled by an electromagnetic brake system. N. Hamzah et al (2007) designed a traditional SMC without including the dynamics of the hydraulic brake and presented digital simulation results with ABS. Design of a conventional SMC based ABS controller with a Sliding Mode Observer (SMO) is discussed by Unsal and Kachroo (1999). The SMC controller is first designed to regulate the wheel slip and then the SMO is designed to estimate the vehicle velocity. S. Drakunov et al (1995) treated the SMC design in a different manner than the approach based on the separation principle. The problem is considered in two steps: first the optimal slip is estimated and then this is treated as a tracking problem relating to that optimal value. An adaptive SMC controller for vehicle traction is considered by A. El Hadri et al (2002). The relative velocity between the vehicle velocity and wheel velocity (named slip velocity) is used as the controlled variable instead of the relative slip. The adaptive law combines conventional SMC and estimation of the tyre/road friction coefficient. The overall system stability is proven by the Lyapunov theory. A robust SMC controller in combination with Neural Networks (NN) is presented by Y. Jing et al (2009). M. Wu et al (2001) presented a method integrating the SMC and Pulse Width Modulation (PWM) for slip control. This work was extended and compared with convectional SMC in M. Wu et al (2003)

This paper is structured as follows. Section 2 presents a full-vehicle nonlinear model used for testing and a corresponding quarter car model that is used for controller design. An optimal slip trajectory generator is presented in Section 3. Then a conventional SMC controller design is implemented in conjunction with a sliding mode differentiator to estimate longitudinal velocity to improve the overall performance in section 4. In section 5 the new TV-SMC controller design is presented. Finally concluding remarks and future work are addressed in section 6.

## 2. MATHEMATICAL MODELS

### 2.1 Nonlinear full -vehicle Model

This model is based on a prototype vehicle and is used to test the designed controllers before they are tested with the industrial simulation platform CarMaker prior to experimental testing on a vehicle.

$$\dot{v}_x = 1/m [(F_x^{fL} + F_x^{fR}) \cos \delta - (F_y^{fL} + F_y^{fR}) \sin \delta + (F_x^{rL} + F_x^{rR}) + \dot{\phi} v_x], \quad (1)$$

$$\dot{v}_y = 1/m [(F_y^{fL} + F_y^{fR}) \cos \delta + (F_x^{fL} + F_x^{fR}) \sin \delta + (F_x^{rL} + F_x^{rR}) - \dot{\phi} v_y] \quad (2)$$

$$\ddot{\phi}_x = 1/I_\phi [L_f (F_x^{fL} + F_x^{fR}) \sin \delta - L_f (F_y^{fL} + F_y^{fR}) \cos \delta + L_f (F_x^{rL} + F_x^{rR})] \quad (3)$$

$$+ [L_w/2 (F_x^{fL} - F_x^{fR}) \cos \delta - L_w/2 (F_y^{fL} - F_y^{fR}) + L_w/2 (F_x^{rL} - F_x^{rR}) \sin \delta].$$

The heave, pitch and roll motions of the vehicle body are included. The lateral and longitudinal velocities of the vehicle are  $v_x$  and  $v_y$ , respectively and the yaw rate,  $\dot{\phi}$ .  $v$  is the vehicle velocity and  $\delta$  is the front wheel steering angle. The lengths  $L_f$  and  $L_r$  refer to the longitudinal distance from the centre of gravity to the front wheels and to the rear wheels, respectively, and  $L_w$  is track width. Let the longitudinal and lateral tire forces be given by  $F_x^{ij}$  and  $F_y^{ij}$ , respectively. The superscript or subscript  $i = fR$  indicates the front and rear, while the superscript or subscript  $j = lR$  indicates the left and right tyres, respectively.

$$\ddot{z}_s = \frac{1}{m_b} [mg - K_f z_s^{fL} - B_f \dot{z}_s^{fL} - K_f z_s^{fR} - B_f \dot{z}_s^{fR}] \quad (4)$$

$$- [K_r z_s^{rL} - B_r \dot{z}_s^{rL} - K_r z_s^{rR} - B_r \dot{z}_s^{rR}]$$

$$\ddot{\theta} = \frac{h_f}{I_\theta} (F_x^{fL} + F_x^{fR}) \cos \delta + (F_y^{fL} + F_y^{fR}) \sin \delta - h_r (F_x^{rL} + F_x^{rR}) - L_f (K_f z_s^{fL} + B_f \dot{z}_s^{fL} + K_f z_s^{fR} + B_f \dot{z}_s^{fR}) \quad (5)$$

$$+ L_r (K_r z_s^{rL} - B_r \dot{z}_s^{rL} - K_r z_s^{rR} - B_r \dot{z}_s^{rR})$$

$$\ddot{\phi} = \frac{h_f}{I_\phi} (F_y^{fL} - F_y^{fR}) \sin \delta + (F_x^{fL} - F_x^{fR}) \cos \delta$$

$$+ h_r (F_x^{rR} - F_x^{rL}) - \frac{L_w}{2} (K_f z_s^{fR} + B_f \dot{z}_s^{fR} + K_r z_s^{rR} + B_r \dot{z}_s^{rR}) \quad (6)$$

$$+ \frac{L_w}{2} (K_f z_s^{fL} + B_f \dot{z}_s^{fL} + K_r z_s^{rL} + B_r \dot{z}_s^{rL})$$

$$\text{where } z_s^{fL} = z_s + I_f \theta + I_w \phi / 2, z_s^{fR} = z_s + I_f \theta - I_w \phi / 2,$$

$$z_s^{rL} = z_s - I_f \theta + I_w \phi / 2, z_s^{rR} = z_s - I_f \theta - I_w \phi / 2,$$

$$\dot{z}_s^{fL} = \dot{z}_s + I_f \dot{\theta} + I_w / 2 \dot{\phi}, \dot{z}_s^{fR} = \dot{z}_s + I_f \dot{\theta} - I_w / 2 \dot{\phi},$$

$$\dot{z}_s^{rL} = \dot{z}_s - I_f \dot{\theta} + I_w / 2 \dot{\phi}, \dot{z}_s^{rR} = \dot{z}_s - I_f \dot{\theta} - I_w / 2 \dot{\phi}$$

The above equations describe the vertical motion of the vehicle. Let  $z_s$  and  $z_s^{ij}$  denote the vertical displacement of the body at the centre and the corner, respectively,  $z_r^{ij}$  the road profiles,  $\theta$  is the body pitch angle,  $m_b$  is the mass of the vehicle without the mass of the front and rear wheels  $m_i^{ij}$ ,  $F_N$  is the normal tyre force, and  $h_i$  is the vertical distance from the centre of gravity to the centre of the front and the rear wheel at equilibrium. The spring and damping constants  $K_i$  and  $B_i$ , respectively, are the lumped parameters associated with the passive suspension system. The state vector of the model is given as

$$x(t) = [v_x \ v_y \ \varphi \ \dot{\phi} \ z_s \ \dot{z}_s \ \theta \ \dot{\theta} \ \phi \ \dot{\phi} \ F_x^{fL} \ F_y^{fL} \ F_x^{fR} \ F_y^{fR} \ F_x^{rL} \ F_y^{rL} \ F_x^{rR} \ F_y^{rR}]^T \quad (7)$$

$$u(t) = [T_b^{fL} \ T_b^{fR} \ T_b^{rL} \ T_b^{rR}]$$

## 2.2 Quarter Car Model

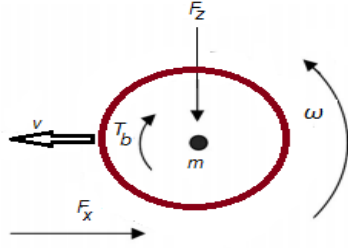


Fig.1. Quarter car

Fig.1 Illustrates the free body diagram of a quarter car vehicle model or single wheel model of a vehicle in longitudinal braking motion. This model captures the fundamental dynamic characteristics of the system in a simple form and it is widely used by control engineers and researchers. The dynamic equations are given as ,

$$J \dot{\omega} = r F_x - T_b \quad (8)$$

$$m \dot{v} = -F_x \quad (9)$$

$$F_x = F_z \mu(\lambda) \quad (10)$$

$J$  is the inertia of the wheel,  $\omega$  is the angular velocity of the wheel,  $F_x$  and  $F_z$  are the friction and normal force acting on wheel respectively,  $v$  is the vehicle velocity,  $T_b$  is the braking torque,  $\mu$  is the tyre-road friction coefficient and  $\lambda$  is the relative wheel slip which is given as follows

$$\lambda = \frac{v - \omega r}{v} \quad (11)$$

Hence, the slip dynamic equation can be derived as follows

$$\dot{\lambda} = \frac{-1}{v} \left( \frac{1-\lambda}{m} + \frac{r^2}{J} \right) F_z \mu(\lambda) + \frac{r}{vJ} T_b \quad (12)$$

## 3. OPTIMAL SLIP GENERATION

One of the objectives of an ABS system is to reduce the braking distance by maximizing the braking force. However, the maximum braking force that could be generated varies with the road conditions. The desired or the optimal slip to provide a maximum braking force is dependent upon the tyre-road friction coefficient. Hence, in reality, optimal slip varies continuously with changing road condition. The Magic Formula (MF) or Pacejka model is used to describe the tyre-road interaction. It is a widely used tyre model to calculate the steady-state tyre forces and moments, H. B. Pacejka, et al (2002). It is a semi-empirical model and is given as follows

$$y(x) = D \sin[C \arctan Bx - E(Bx - \arctan Bx)] \quad (13)$$

where

$B$  = Stiffness factor,  $C$  = Shape factor,  $D$  = Peak value,  $E$  = Curvature factor.

The maximum braking force will be generated at the optimal slip  $\lambda^d$ . Therefore, one can find,

$$\frac{dy}{dx} \Big|_{(x=\lambda^d)} = 0 \quad (14)$$

From the Magic formula, it follows that

$$\frac{dy}{dx} = \frac{BCD}{(1+[Bx(1-E)+E \arctan(Bx)]^2)} \quad (15)$$

$$[1-E + \frac{E}{(1+B^2x^2)}] \cos C \arctan [Bx(1-E)+E \arctan(Bx)]$$

Equations (14) and (15) yield

$$\cos C \arctan [B \lambda^d (1-E) + E \arctan(B \lambda^d)] = 0 \quad (16)$$

Therefore, the optimized slip can be expressed as

$$\lambda^d = \frac{\tan(0.5)\pi / C - E \arctan(B \lambda^d)}{B(1-E)} \quad (17)$$

The magic formula optimization is given in Fig.2.

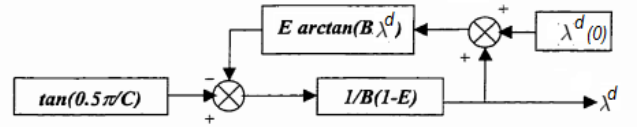


Fig.2. Magic Formula Optimisation

The shape coefficients  $B, C, D, E$  of the Magic formula depend on the road conditions and should be updated. Typically an Extended Kalman Filter (EKF) is used to update the coefficients. The corresponding equations are given below.

The system is defined as

$$x_{k+1} = f(a_k, u_k) + w_k, a_{k+1} = a_k + \xi_k, z_k = h(a_k) + v_k \quad (18)$$

For this system, the parameters  $a_k$  can be estimated by means of the following equations,

$$a_{k+1} = a_k, p_{k+1}^- = s_k \quad (19)$$

The measurement update:

$$k_k = p_k^- H_k^T (H_k p_k^- H_k^T + R_k)^{-1}, \hat{a}_k = \hat{a}_k^- + K_k (z_k - h(\hat{a}_k^-))$$

$$p_k = (1 - K_k H_k) p_k^- \quad (20)$$

where  $H_k = \frac{dh(\hat{a}_k)}{da}$ , and the parameters in this model are defined as

$$C_x = \rho_{c_{x1}}, D_x = \mu_x F_z, E_x = \rho_{E_{x1}} + \rho_{E_{x2}} df_z + \rho_{E_{x3}} df_z^2 \quad (21)$$

$$B_x = F_z (\rho_{K_{x1}} + \rho_{K_{x2}} df_z) \exp(\rho_{K_{x3}} df_z) / (C_x D_x)$$

#### 4. SLIDING MODE CONTROL

SMC design consists of two steps. First, a sliding surface is designed to define the desired closed loop system performance. Secondly, a control law is derived to drive the system states towards the designed sliding surface and subsequently ensure that the states stay on the surface. The traditional SMC controller developed to track the optimal slip in this section is similar to the one presented by M. Schinkel et al (2002) and E. Kayacan et al (2009).

The switching function or the sliding surface is chosen as follows

$$s = \lambda - \lambda_d \quad (22)$$

This is because  $\lambda_d$  is the slip ratio that provides maximum friction force and the error equation of slip ratio is defined as  $e = \lambda - \lambda_d$ , so the controller should try to minimize this error. The sliding motion occurs when the states reaches the sliding surface defined by  $s = 0$ . The control effort required, on average, to maintain the states on the sliding surface is termed the equivalent control and here it is name equivalent brake torque,  $T_{eq}$ . The dynamics in the sliding motion satisfy

$$\dot{s} = 0 = \dot{\lambda} - \dot{\lambda}_d \quad (23)$$

Then by substituting (13) in (23) and assuming the optimal slip is constant, it follows that

$$0 = \frac{1}{v} \left[ \frac{-r}{J} (F_x r - T_b) + (1 - \lambda) \dot{v} \right] \quad (24)$$

Solving for the equivalent brake control torque,  $T_{eq}$ , it is obtained that

$$T_{eq} = F_x r - (1 - \lambda) \frac{\dot{v} J}{r} \quad (25)$$

If the system states are not on the sliding surface, or the system experience uncertainty or disturbances, then an additional control torque  $T_{bh}$  is required.  $T_{bh}$  is determined by the following reaching condition

$$s \dot{s} \leq -\eta_s |s| \quad (26)$$

where  $\eta$  is strictly positive design parameter. Using (22) and (24), (26) can be rewritten as

$$s \dot{\lambda} \leq -\eta_s |s| \quad (27)$$

Substitution of (24) into (27) results in

$$\frac{s}{v} \left( \frac{-r}{J} (F_x r - (T_{beq} - T_{bh} \text{sgn}(s))) + (1 - \lambda) \dot{v} \right) \leq -\eta_s |s| \quad (25)$$

Solving (25) to obtain  $T_{bh}$  results in

$$T_{bh} = \frac{vJ}{r} (F + \eta_s) \quad (26)$$

where  $F \geq ((1 - \lambda) \dot{v} - \hat{v})$  and  $\hat{v}$  is the estimate of the vehicle longitudinal acceleration. This is estimated by an EKF. The overall torque  $T_b$  can be expressed as

$$T_b = T_{beq} - T_{bh} \text{sgn}(s) \quad (27)$$

To eliminate the chattering problem the discontinuous switching function is replaced by the continuous function given by

$$f(s) = \frac{s}{|s| + \delta} \quad (28)$$

where  $\delta > 0$ . Therefore, the total brake torque  $T_b$  is given by

$$T_b = F_x r - (1 - \lambda) \frac{\hat{v} J}{r} - \frac{vJ}{r} (F + \eta_s) f(s) \quad (29)$$

The experimental vehicle used is a Delta car with two traction Electric Motors (EMs) that have been re-purposed to facilitate braking and slip control is shown in Fig.3.



Fig.3 Experimental Vehicle

The vehicle starts to accelerate from standing to reach the target test speed before entering the gravel road. When the vehicle enters the lane, the driver stops accelerating. The braking is initiated by the passenger, by pressing a virtual button on a PC.

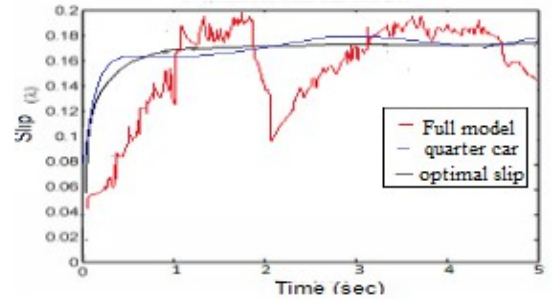


Fig.4 Full car and quarter car model slip responses

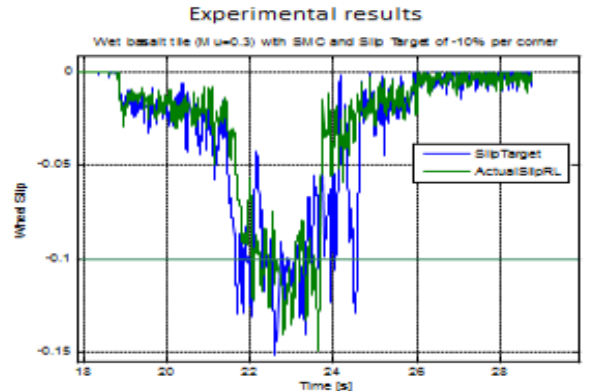


Fig.5. Experimental slip response

The simulation results with the quarter car model and fully nonlinear car model as well as experimental results are given in Fig.4 and 5 respectively. It can be seen that the experimental results exhibit a very oscillatory response compared to both sets of simulation results. The differences are thought likely to be caused by ineffective estimation of longitudinal velocity  $v$  by EKF.

The use of a Sliding Mode Differentiator (SMD) to estimate  $v$  is considered in the following subsection.

#### 4.1 Sliding Mode Differentiator (SMD)

The SM differentiator toolbox developed by M. Reichhartinger and S.K. Spurgeon (2016) is used here to estimate the longitudinal velocity and the results are compared with the response of the EKF. The differentiator block is presented in Fig.8. The higher order SMD was found to produce a better estimate of the longitudinal velocity. It can be seen in Fig.9 that the higher the order of the differentiator, the better is the response produced.

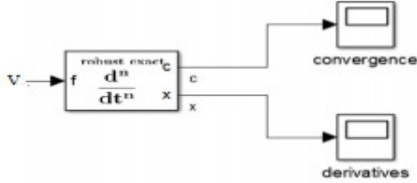


Fig.8. Differentiator Block

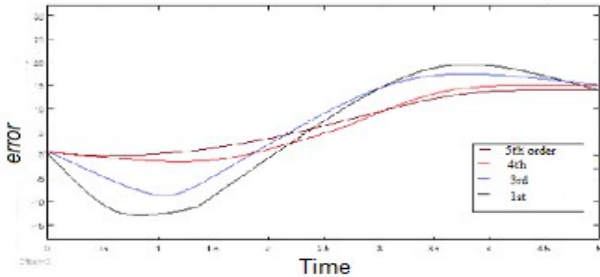


Fig.9 Responses obtained with higher orders of SMD

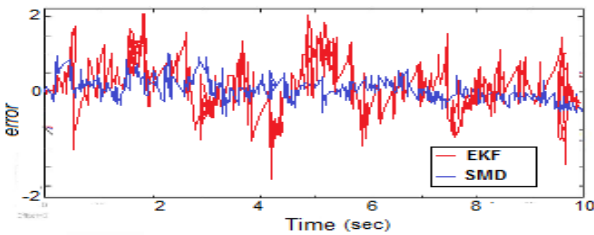


Fig.10. EKF and SMD error in estimation of  $v$

The velocity response from the SMD is compared with the EKF and shown in Fig.10. The SMD produced a much better result when compared to the EKF.

### 5. TV-SMC CONTROLER

The SMC controllers presented in the literature for ABS operation in braking are frequently based on constant optimal desired slip corresponding to particular surface conditions.

However, in operation this assumption does not hold and the optimal slip changes with time. This motivates including time-varying optimal slip in the controller design paradigm. Here the development of an SMC with a time-varying surface to track an optimal trajectory during braking is considered.

The system described in (12) is written in the form of

$$\dot{x} = f(x) + bu, y = x = \lambda \quad (30)$$

where  $f(x) = -\frac{1}{v}(\frac{F_x}{m}(1-\lambda) + \frac{rF_x}{J})$ ,  $b = \frac{r}{vJ}$  and  $u = T_b$ .

$f(x)$  is a nonlinear function and includes uncertainties which should be estimated. The control objective is to track the desired slip trajectory,

$$x_d = \lambda_d = [x_{1d}, x_{2d}, \dots, x_{nd}]^T \quad (31)$$

So the slip error is expressed as

$$e = x - x_d = [x_1 - x_{1d}, \dots, x_n - x_{nd}]^T \quad (32)$$

The new time-varying sliding surface is defined as

$$\sigma(x; t) = \left(\frac{d}{dt} + k\right)^{(n-1)} e \quad (33)$$

$$\sigma(x; t) = \Lambda^T e$$

where  $\Lambda = [k^{n-1} \ (n-1)k^{n-2} \ \dots \ k]$  and  $k$  is a positive value selected based on the road conditions. The positive definite Lyapunov function candidate is chosen as

$$V(\sigma) = \frac{1}{2} \sigma^T \sigma = \frac{1}{2} e^T \Lambda \Lambda^T e \quad (34)$$

$V(\sigma)$  guarantees that the error state converges to the sliding surface if the following condition holds

$$\dot{V}(\sigma) = \sigma \dot{\sigma} < 0 \quad (35)$$

Choosing  $\dot{\sigma} = \eta \text{sign}(\sigma)$  and  $\eta > 0$ , it follows

$$\dot{\sigma} = \Lambda^T \dot{e} = \Lambda^T (f(x) + bu - \dot{x}_d) = -\eta \text{sign}(\sigma) \quad (36)$$

Hence the control  $u$  is derived as follows

$$u = (\Lambda^T b)^{-1} [\Lambda^T \dot{x}_d - \Lambda^T \hat{f}(x) - \eta \text{sign}(\sigma)], (\Lambda^T b) \neq 0 \quad (37)$$

where  $\hat{f}(x)$  is an estimate of nonlinear function  $f(x)$ . If  $f(x)$  is available, then  $\dot{\sigma}$  can be written as

$$\dot{\sigma} = -\eta \text{sign}(\sigma) - \Lambda^T (f(x) - \hat{f}(x)) \quad (38)$$

where  $\Delta f(x)$  is the estimation error for the function  $f(x)$  and it is assumed that it can be bounded by a known function  $F = F(x)$  and  $|\hat{f}(x) - f(x)| \leq F$ .

Differentiation of the Lyapunov function candidate with respect to time yields

$$\dot{V}(\sigma) = \sigma \dot{\sigma} = -\eta \sigma \text{sign}(\sigma) + \sigma \Lambda^T \Delta f(x) \quad (39)$$

$$\dot{V} = -\eta |\sigma| + \sigma \Lambda^T \Delta f(x)$$

The  $\sigma$ -dynamics can be made globally asymptotically stable from (39) if  $\eta$  is chosen as



$$\eta > \|A^T\| \cdot \|\Delta f(x)\| \quad (40)$$

Choosing  $\eta$  according to (40) ensures that  $\dot{V}(\sigma) < 0$ . Hence, according to Barbalat's lemma  $\sigma$  converges to zero in finite time if  $\eta$  is chosen large enough to overcome the destabilizing effects of the unmodeled dynamics  $\Delta f(x)$ .

To prevent chattering caused by the discontinuity in the control law, the sign function can be replaced by the continuous function  $\tanh(\sigma/\phi)$ , where  $\phi$  is the sliding surface boundary layer thickness. Reducing  $\phi$  increases the nonlinear gain, while increasing  $\phi$  introduces a filtering effect if measurements are noisy. So the proposed control law is given by

$$u = (A^T b)^{-1} [A^T \dot{x}_d - A^T \hat{f}(x) - \eta \tanh(\sigma/\phi)] \quad (41)$$

The controller is tested with nonlinear full car model and the results are given below.

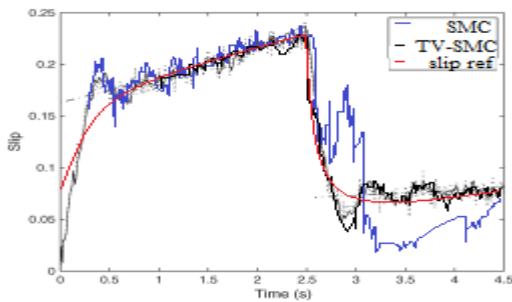


Fig.11. TV-SMC and SMC varying slip tracking response

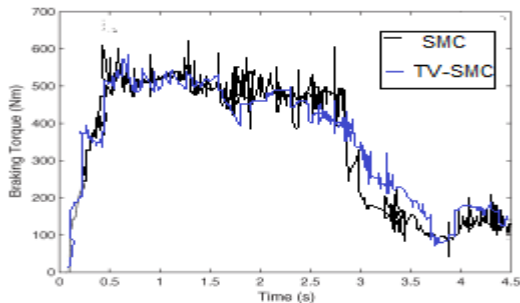


Fig.12. Braking torques of TV-SMC and SMC

## 6. CONCLUSIONS

Many different control approaches have been previously applied to the ABS problem. Most model based approaches fail to exhibit the required level of adaptability and robustness to varying road surface conditions in practice. The proposed TV-SMC produced better results when compared to a classical SMC. However, tuning of the TV-SMC is time consuming and the positive value  $k$  is selected by linearising the model at different local points corresponding to various tyre-road conditions. The proposed SMD produced a much better estimate of  $v$  when compared to the EKF. Testing of both the TV-SMC and SMD on an experimental vehicle will be the subject of future work. Furthermore, sliding mode observers will be designed to estimate the longitudinal vehicle velocity and friction.

## REFERENCES

- K. Chun, M. Sunwoo, (2002) "Wheel slip control with moving sliding surface for traction control system", *International Journal of Automotive Technology*, Vol. 5, No. 2, pp. 123-133.
- S. Drakunov, U. Ozguner, P. Dix, B. Ashrafi, (1995) "ABS control using optimum search via sliding modes", *IEEE Transactions on Control Systems Technology*, Vol. 3, No. 1, pp. 79-85.
- A. El Hadri, J. C Cadiou, N. K. M'sirdi, (2002) "Adaptive sliding mode control of vehicle traction", *15th Triennial World Congress*.
- N. Hamzah, M.Y. Sam, A. A. Basari, (2007) "Enhancement of driving safety feature via sliding mode control approach", *Fourth International Conference on Computational Intelligence, Robotics and Autonomous Systems*, pp. 116-120.
- Y. Jing, Y. Mao, G. M. Dimirovski, Y. Zheng, S. Zhang, (2009) "Adaptive global sliding mode control strategy for the vehicle antilock braking systems", *American Control Conference*, pp. 769-773.
- E. Kayacan, Y. Oniz, O. Kaynak, (2009) "A grey system modeling approach for sliding-mode control of antilock braking systems", *IEEE Transactions on Industrial Electronics*, Vol.56, No.8, pp. 3244-3252.
- Y. Oniz, E. Kayacan, O. Kaynak, (2007) "Simulated and experimental study of antilock braking system using grey sliding mode control", *ISIC. IEEE International Conference on Systems, Man and Cybernetics*, pp. 90-95.
- H. B. Pacejka, (2002) *Tyre and Vehicle Dynamics*, 3rd ed. Butterworth-Heinemann ch. 4.
- E. J. Park, D. Stoikov, L. Falcao da Luz, A. Suleman, (2006) "A performance evaluation of an automotive magnetorheological brake design with a sliding mode controller", *Mechatronics*, Vol. 16, No. 7, pp. 405-416.
- M. Reichhartinger and S.K. Spurgeon (2016) "A Robust Exact Differentiator Block for MATLAB R / Simulink" R DOI: ..., Technical University of Graz.
- M. Schinkel and K. Hunt, (2002) "Anti-lock braking control using a sliding mode approach," in *Proc. Amer. Control Conf.*, Anchorage, AK, pp. 2386-239.
- J. Song, "Performance evaluation of a hybrid electric brake system with a sliding mode controller", *Mechatronics*, Vol. 15, No. 3, pp. 339-358.
- C. Unsal, P. Kachroo, (1999) "Sliding mode measurement feedback control for antilock braking systems", *IEEE Transactions on Control Systems Technology*, Vol. 7, No. 2, pp. 271-281.
- M. Wu, M. Shih, "Simulated and experimental study of hydraulic anti-lock braking system using sliding-mode PWM control", *Mechatronics*, Vol. 13, No. 4, pp. 331-351.
- M. Wu, M. Shih, (2001) "Using the sliding-mode pwm method in an anti-lock braking system", *Asian Journal of Control*, Vol. 3, No. 3, pp. 255-261.